Life Cycle Characteristics of Deep Cloud Systems over the Indian Region Using *INSAT-1B* Pixel Data

ARVIND V. GAMBHEER AND G. S. BHAT

Centre for Atmospheric and Oceanic Sciences, Indian Institute of Science, Bangalore, India

(Manuscript received 22 November 1999, in final form 1 May 2000)

ABSTRACT

A detailed study of deep cloud systems (denoted by CSs) over the Indian region using *INSAT-1B* pixel data is presented. The life cycle characteristics of CSs are examined, including their preferred regions of formation and dissipation, frequency of occurrence, life duration, and speeds of propagation. A new automatic algorithm to track cloud systems has been developed that takes into account the mergers and splits in CSs. The algorithm is based on a combination of the maximum allowable displacement of a CS in 3 h and area overlap. The choice of the minimum size for CS is fixed at 4800 km^2. The temperature threshold is varied from 201 to 261 K. It is observed that majority of CSs decay within a couple of hundred kilometers from where they form. There is a bimonthly modulation of the areal extent of more frequent convection. The number of CSs increases approximately linearly with threshold temperature up to 251 K. Tracking results are not very sensitive to the criterion chosen for identifying the successor in cases of multiple candidates, except for CSs that live longer than 36 h. Mean speeds of propagation of CSs range from 7 to 9 m s^{-1}.

1. Introduction

Clouds in the tropical atmosphere occur in a wide range of sizes starting from isolated cumulus to large cloud clusters. The latter exhibit mesoscale organization and account for most of the vertical transport of energy from the planetary boundary layer to the upper troposphere and rainfall (e.g., Williams and Houze 1987). The stratiform cloud shield associated with the cloud clusters heats the upper atmosphere by trapping the radiation (Webster and Stephens 1980). Thus, the cloud clusters are an important phenomenon associated with weather and climate. Their study is necessary to improve the forecasting on short and long timescales, and for understanding climate and its variability and the general circulation of the atmosphere.

In the present study, the terms cloud cluster, cloud system (CS), and mesoscale convective system (MCS) are all considered to refer to the same phenomenon, namely, deep convective cloud systems. Much of the present understanding of the structure and dynamics of MCSs has come from radar observations (e.g., Houze and Cheng 1977; Mapes and Houze 1995). An active MCS simultaneously contains growing and matured convective cells (Cb clouds) along with a large stratus anvil cloud formed by the merger of older and outflow from active Cb clouds (Houze 1989). The matured Cb clouds are the tallest, often reach the tropopause level, and the height of the anvil cloud gradually decreases away from active convective cells. Thus, an important characteristic feature of MCS is that it contains clouds whose tops are at different vertical levels. In a typical MCS, about 10% of the area is covered by the convective cells and the remainder by the anvil clouds (Houze 1993, chapter 9). MCSs are not stationary and move with speeds ranging from a few meters per second to 25 m s^{-1} (e.g., Barnes and Sieckman 1984; Corfidi et al. 1996).

The spatial coverage of radars is limited and only satellites provide information about the clouds globally. While radars detect the hydrometeors in clouds, the satellites measure the radiance (reflected and emitted) from the earth–atmosphere system. Deep clouds are identified from the low values of brightness temperature in IR imagery. Using the geostationary satellite data in particular (which are available at regular time intervals, typically after every 1.5–3.0 h), it became possible to study various aspects of deep clouds, including their seasonal geographic distributions and life cycle characteristics. For example, Aspliden et al. (1976) manually tracked the disturbance lines over eastern Atlantic and West Africa for the Global Atmospheric Research Program (GARP) Atlantic Tropical Experiment period and found that more than 77% of the disturbance lines' activity was over land. The speeds of propagation of dis-

Corresponding author address: Dr. G. S. Bhat, Center for Atmospheric and Oceanic Studies, Indian Institute of Sciences, Bangalore 560 012, India.
E-mail: bhat@caos.iisc.ernet.in

turbance lines ranged from 20 to 120 km h^{-1}. Martin and Schreiner (1981) manually tracked the clouds and studied size, intensity, trajectories, lifetimes, and distributions of cloud clusters over West Africa and the eastern Atlantic Ocean. They observed that, in general, cloud lifetime increased with its size. Williams and Houze (1987) developed an automated method for tracking clouds and applied it for studying clouds during the Winter Monsoon Experiment carried out in the region near the south China Sea and Borneo. Williams and Houze (1987) observed that the size distribution of cloud clusters was a truncated lognormal type and most of the cumulative cloud cover was accounted for by a few large clusters.

The unique advantage of geostationary satellites in providing information on clouds over large spatial and long temporal scales with fine spatiotemporal resolution is demonstrated in the study of Nakazawa (1988). Nakazawa (1988) used 3-hourly Geostationary Meteorological Satellite IR data for the region 60°N to 60°S and 80°E to 180°, and showed that within the intraseasonal oscillation there were several superclusters with a horizontal length scale of several thousands of kilometres and with timescale of less than 10 days moving eastward with a speed of 10–15 m s^{-1}. Within superclusters, there were two to three cloud clusters of 100-km horizontal scale and 1–2-day timescale moving westward. Machado and Rossow (1993) found that (on a global scale) CSs occurred more frequently on land than over ocean and that on land the smallest CSs occurred more frequently and that the largest appeared less frequently than over oceans.

Machado et al. (1998) studied the life cycle characteristics of MCS over the Americas using *Geostationary Operational Environmental Satellite-7* and International Satellite Cloud Climatology Program B3 satellite data for the period 1987–88. This study used 26 parameters for each possible pair (like location of clouds, their radii, average, minimum, variance and gradient of cloud-top temperature and reflectance, eccentricity, and inclination of axis) and the different combinations of the parameters differences to determine a match or a lack of one. They used both semiautomatic (manual) and automatic algorithms for tracking clouds. The average propagation speed was 12 m s^{-1} for semiautomatic tracking and 17 m s^{-1} for the automatic tracking. Further, compared to the semiautomatic algorithm, the number of systems recognized by the automatic algorithm was larger by 50%. Thus the results are sensitive to the method of tracking.

The diurnal variation in convective activity is another aspect that has been extensively studied using satellite data (e.g., Duvel 1989; Chen and Houze 1997; Hall and Vonder Haar 1999). It has been found that deep convective activity peaks during certain periods of the day. For example, over the landmass, convection peaks during late afternoon and evening hours, and over oceans, early morning is the preferred time (Chen and Houze 1997; Hall and Vonder Haar 1999).

Thus, satellite data are very useful sources of information on clouds, and they have enabled the study of several aspects of deep clouds on a wide range of spatiotemporal scales. If we consider the regions of the Tropics covered by the previous studies, the Indian region stands out as the least studied area (by the Indian region we mean the Indian subcontinent and the tropical Indian Ocean). The Indian region is special because of the asymmetry in the distribution of landmass between the Northern and Southern Hemispheres and the large northward migration of the cloud band during the Indian summer monsoon. Therefore, the region is ideal for understanding seasonal and land–sea contrasts. Further, the sea surface temperatures in the Indian Ocean are among the warmest on the globe (Slutz et al. 1985) favoring the high frequency of deep convection throughout the year. A systematic and detailed study of deep cloud systems has been missing for the Indian region; the only study to our knowledge is that of Laing and Fritsch (1993), which considered mesoscale convective complexes (MCCs), which are large CSs satisfying certain shape requirements (Maddox 1980). The constraints on minimum area and elliptic shape severely restrict the number of systems that qualify as MCCs, and many systems, which are large and perhaps dynamically as important as MCCs, might have been omitted. As shown later in this paper, our results confirm this.

The present study is aimed at understanding the life cycle characteristics of deep CSs in the Indian region without constraining them with specific shape requirements. The emphasis is on broad features covering a wide range of threshold temperatures (201–261 K) and sizes (from 4840 km^2 onward). Another important objective is to identify the preferred regions of formation and dissipation of convective systems; such information is useful, for example, in deciding the locations for enhanced field observations and ground truths. A new automated tracking algorithm is developed for the purpose. The method is based on the combination of maximum permissible movement of CSs and area overlap. The paper is organized as follows. In section 2 the satellite data are briefly described, section 3 contains the details of the tracking algorithm and results are presented in section 4. Section 5 has conclusions.

2. Data

The present study is based on the 3-hourly infrared *INSAT-1B* data archived at the National Center for Atmospheric Research, Boulder, Colorado. The study period is from April 1988 to March 1989 and the area of interest is 30°S to 30°N and 40° to 110°E (Fig. 1). Figure 1 also shows the area correction factors to account for the curvature of the earth's surface and satellite look angle while calculating the actual area of the pixels.

For studying the life cycles of clouds, image sampling

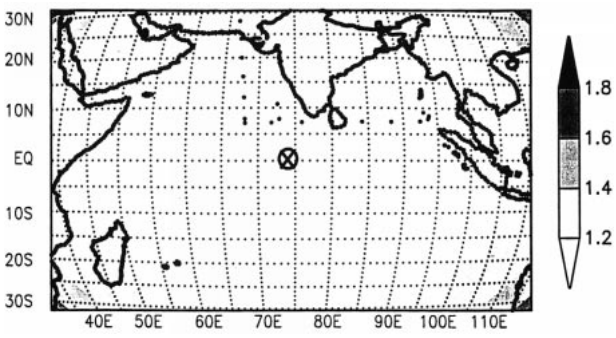

FIG. 1. Study region and the area correction factor, expressed in terms of the equivalent number of standard pixels, to account for the curvature of the earth and satellite look angle while calculating the actual area of a pixel. The encircled × denotes the position of the subsatellite point.

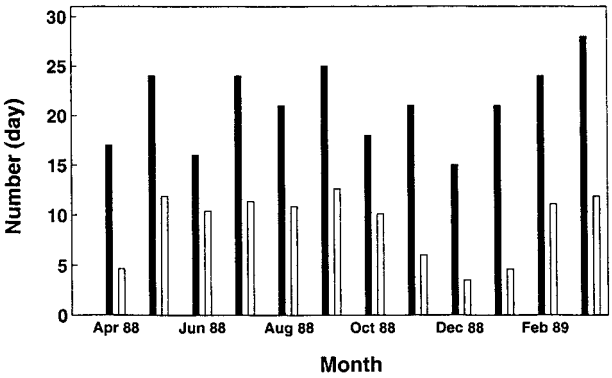

FIG. 2. Number of independent (nonoverlapping) contiguous eight-image stretches (solid bar) and longest span of contiguous images (open bar) expressed in terms of equivalent number of days per month.

time interval and data continuity are very important. Here, IR images are available every 3 h. Deep convective clouds in the atmosphere exist in a wide spectrum of timescales. The typical life cycle of a Cb cloud is about 30 min to 1 h, that of a thunderstorm is a few hours, and the average life of larger MCSs is about 10 h (Ludlam 1980, chapter 8; Houze 1993, p. 337). Therefore, with the sampling time of 3 h, some smaller CSs may not be seen at all, and the life cycles of those living for less than 6 h are poorly resolved. While short-lived, small-sized CSs dominate the cloud population, it is the larger, long-living CSs (life ~ 10 h) that contribute to overall cloud cover and total precipitation (Houze 1993, p. 337). The present sampling time of 3 h is reasonably adequate to study the life cycle characteristics of larger CSs, which have a major impact on weather and climate.

Data continuity is also important since the algorithms that track CSs in successive images terminate all CSs when a missing image is encountered. This results in underestimation of the life duration of some systems that exist at image discontinuity. In the present dataset, some images are missing. Figure 2 shows the number of independent (i.e., nonoverlapping) contiguous eight-image stretches (solid bars) and the longest contiguous stretch of images (open bars) for each month expressed in equivalent number of days per month. Referring to Fig. 2, it is seen that the number of contiguous images exceeds 20 days during 8 months, and for the remaining 4 months, it is more than 15 days. Very often, contiguous images are available for several days at a stretch. It is observed from Fig. 2 that for 8 months the longest continuous stretch of data is between 10 and 13 days, which corresponds to 80–100 images. For the remaining 4 months (viz., April, November, and December of 1988 and January 1989) the longest span is more than 3 days. Thus, there are a number of contiguous image stretches every month that are much longer than the average life cycle of MCSs and the data continuity is reasonable for the study of the life cycle of even long-living MCSs.

3. Methodology

a. Definition of a CS

Here a CS is defined as a set of contiguous pixels whose brightness temperature is equal to or below a specified threshold temperature. A survey of the previous studies reveals that the threshold temperature and minimum size prescribed vary in the definitions of a CS and there is no single or uniformly accepted definition of a CS for a satellite image. The threshold temperature has been varied from 198 K (Mapes and Houze 1993) to 267 K (Fu et al. 1990) and the minimum area from 2000 km^2 (Mohr and Zipser 1996) to 100 000 km^2 (Maddox 1980). In addition, many studies, especially those on MCCs, require that the CS contain pixels at a colder temperature along with certain restrictions on the shape of the cloud (Maddox 1980). It has been observed by Augustine and Howard (1988) that two temperature thresholds are not required for the definition of an MCC.

For the present study area, it was observed that CSs below 10 pixels in size contribute more than 50% in terms of numbers; however, their contribution to the total cloud cover is less than 5%. The minimum size for the CS is specified as 10 pixels in the present study, which corresponds to a minimum area of 4840 km^2 and is comparable to the minimum area of 5000 km^2 used by Williams and Houze (1987). Visual observations reveal that CSs occur in various shapes and constraining them with the specific shape requirements will result in many systems being missed. Therefore, here, no restriction is prescribed on the shape of a CS. The threshold temperature is varied from 201 to 261 K in 10-K steps. The cloud-top heights corresponding to 201- and 261-K threshold temperatures are approximately 15 and 8 km, respectively.

b. Tracking algorithm

During 3 h, a CS can move, grow, decay, change shape, split into, or merge with one or more systems.

A tracking algorithm needs to identify the related CSs in successive images accounting for the above possibilities. Williams and Houze (1987) used the area overlap method for tracking clouds. Their requirement of minimum 50% or 10 000 km^2 area overlap (whichever is minimum) restricts the maximum cloud propagation speeds to about 8 m s^{-1} for smaller-sized systems. Both radar and satellite studies have shown that, for MCSs, propagation speeds of more than 10 m s^{-1} are common in the atmosphere (Corfidi et al. 1996). Thus the algorithm by Williams and Houze (1987) misses faster-moving small systems. The algorithm of Machado et al. (1998) has too many parameters. Our objective was to develop an automatic cloud tracking algorithm that catches fast-moving systems and, at the same time, is less complicated than that of Machado et al. (1998). The tracking method developed here has some features common with the previous tracking techniques like the use of a search box (Machado et al. 1998) and area overlap (Williams and Houze 1987). The steps involved are as follows.

For the specified threshold temperature, CSs are identified first and then arranged in decreasing order of their size (mainly to facilitate manual checking of the tracking results when required) for every frame. A circle of 200-km radius is drawn around the center of gravity (CG) of every CS in the first frame. If the CG of a system in the next frame lies within the circle, it is a candidate for the successor. This corresponds to a maximum cloud propagation speed of about 18 m s^{-1}. If more than one system are present, the following parameter is calculated for all possible successors:

$$\text{PDA} = \delta r \times \delta A,$$

where δr is the displacement of the CG and δA is the difference in the area between the original system and its successor. Basically, PDA takes into account both the movement of the CS and the change in its area. Among the possible candidates, one having minimum PDA is taken as the natural successor. When no natural successor is found, it is possible that the system has decayed, split into two or more systems, or merged with other systems. It is observed that whenever two or more CSs merge or a CS splits, there is a considerable change in area. Further, the CGs of the split/merged systems could be more than 200 km apart from the original CG. Thus, even when a natural successor is found, if there is a large change in the area of the CS between two successive frames, the possibility of merger or split exists. Therefore, whenever a CS does not find a natural successor or it finds one but there is considerable change in the area (taken as 20% or more in the present study), then the subroutine OVERLAP is called. In the subroutine OVERLAP, the pixels of the CS under consideration are projected onto the next frame. The CSs in the next frame having an area overlap of five pixels or more with the original system are taken as possible successors. Following a similar procedure, the CSs that merge and form a big system are identified.

When a big CS breaks up, only one among the split systems is treated as the main successor and the rest are treated as new systems. Similarly, when CSs merge, the new system is treated as the successor of only one CS of the previous frame, and the remaining systems are terminated. In a case of multiple candidates, three criteria are used in choosing the main successor or parent, as the case may be. They are 1) biggest system among the candidates, 2) one having maximum area overlap with the parent–child, and 3) one whose propagation trajectory is nearest to that of parent. The last criterion is applicable for CSs having a minimum life cycle of three images, is similar to that adopted by Evans and Shemo (1996), and is used only in the case of splitting.

The CSs having neither a natural successor by the PDA method nor finding a successor after passing through the OVERLAP program are considered as decayed and are terminated. For a CS having a successor, the successor is identified with its parent and its life history is tracked in successive images till the system decays. A CS that is not related to any CSs in the previous frame is treated as new.

To begin with, the computer code to track CSs based on the above algorithm was run for 1 month at the threshold temperature of 221 K, and the hierarchy of the CSs obtained was printed out. Then all the systems tracked by the code were manually verified to check if the algorithm was correctly implemented. It was observed that the code correctly identified related systems including splits and mergers. Having satisfied that the code works well, it was used for tracking the CSs.

For every CS tracked, time of its formation and dissipation [in local standard time (LST) based on the longitude of its CG], position of CG, the maximum area reached during its life span, and corresponding LST and splits or/and mergers were documented.

4. Results

a. Spatial distribution

To begin with, let us consider the spatial distribution of the locations of formation of CSs during each month for the period of the study. The locations where the 221-K CSs formed are shown in Figs. 3 and 4. In Fig. 3, one-frame systems, that is, CSs seen in only one image, are also included, whereas, in Fig. 4, only those that are tracked in at least two images are considered. The seasonal march of the convection zone is clearly seen from Figs. 3 and 4. There is a clear difference in the spatial distribution of CSs between Northern and Southern Hemispheric summers. During the peak monsoon months (Northern Hemispheric summer) namely, in July, August, and September, the latitudinal extent of the formation of CSs extends from 10°S to beyond 25°N. On the other hand, during January and February, the

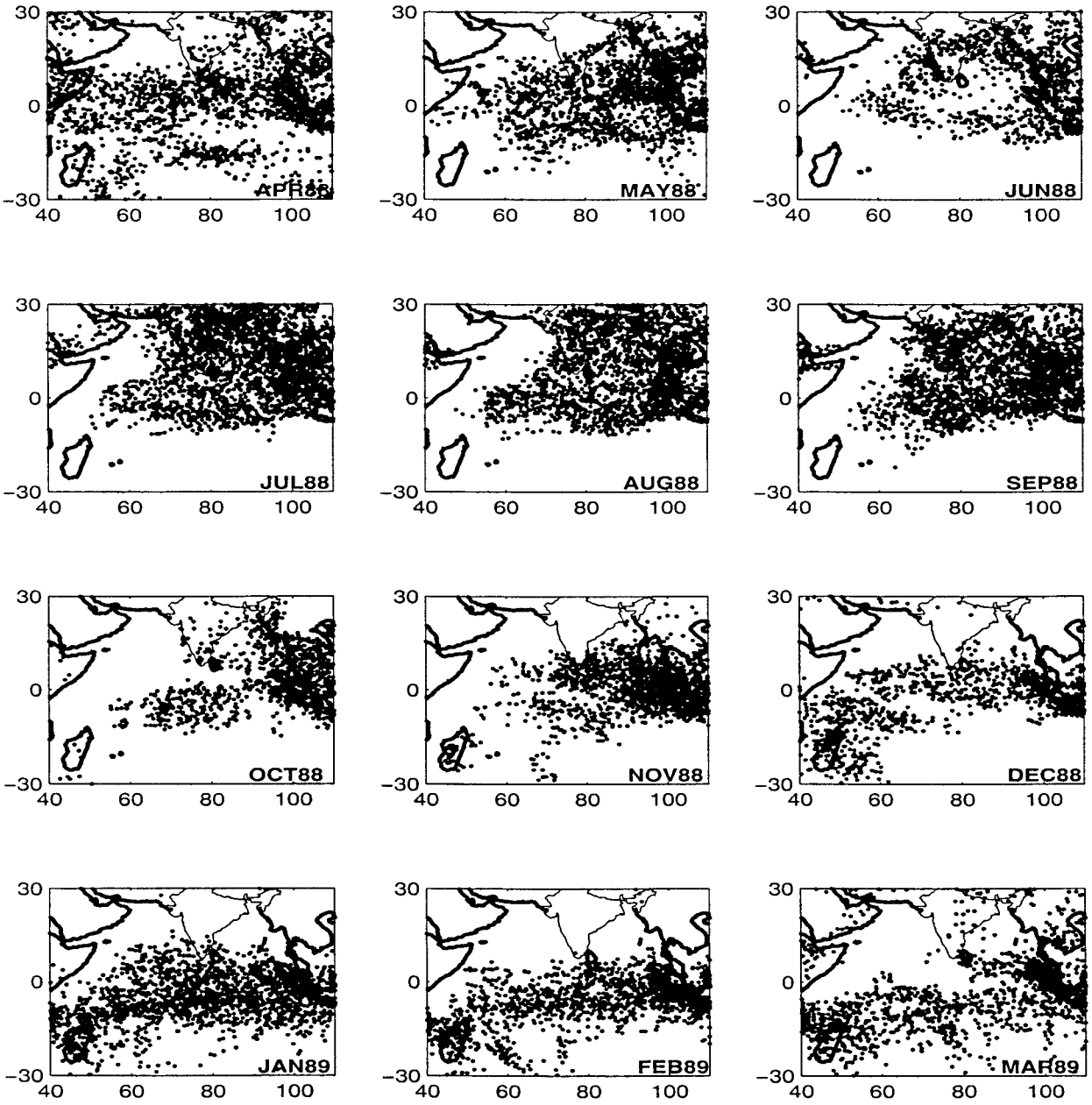

FIG. 3. Monthly distribution of the locations of the 221-K CSs.

distribution is along the zonal belt, and at any longitude, the latitudinal extent is comparatively narrow (Fig. 4). The migration of convection in Figs. 3 and 4 somewhat follows the position of maximum solar heating, suggesting that surface thermodynamic properties modulate convection. Indeed, previous studies have shown that convection depends on SST over oceans (e.g., Gadgil et al. 1984; Graham and Barnett 1987; Fu et al. 1994). We used National Centers for Environmental Prediction (NCEP) daily reanalysis data to study the dependence of convection on surface properties. Since the present study area has substantial landmass, we found that a thermodynamic parameter that combines temperature and humidity is superior to the surface temperature alone in relating convection and surface properties. It was observed that the areas of increased convection had larger values of moist static energy h at the surface (h is defined as $h = C_pT + gz + Lq$, where C_p is specific heat of air at constant pressure, T is air temperature, g is acceleration due to gravity, z is geopotential height, L is the latent heat of evaporation, and q is water vapor mixing ratio). However, the overall correlation between h and convection was not high, as there were also areas with high moist static energy with little or no convec-

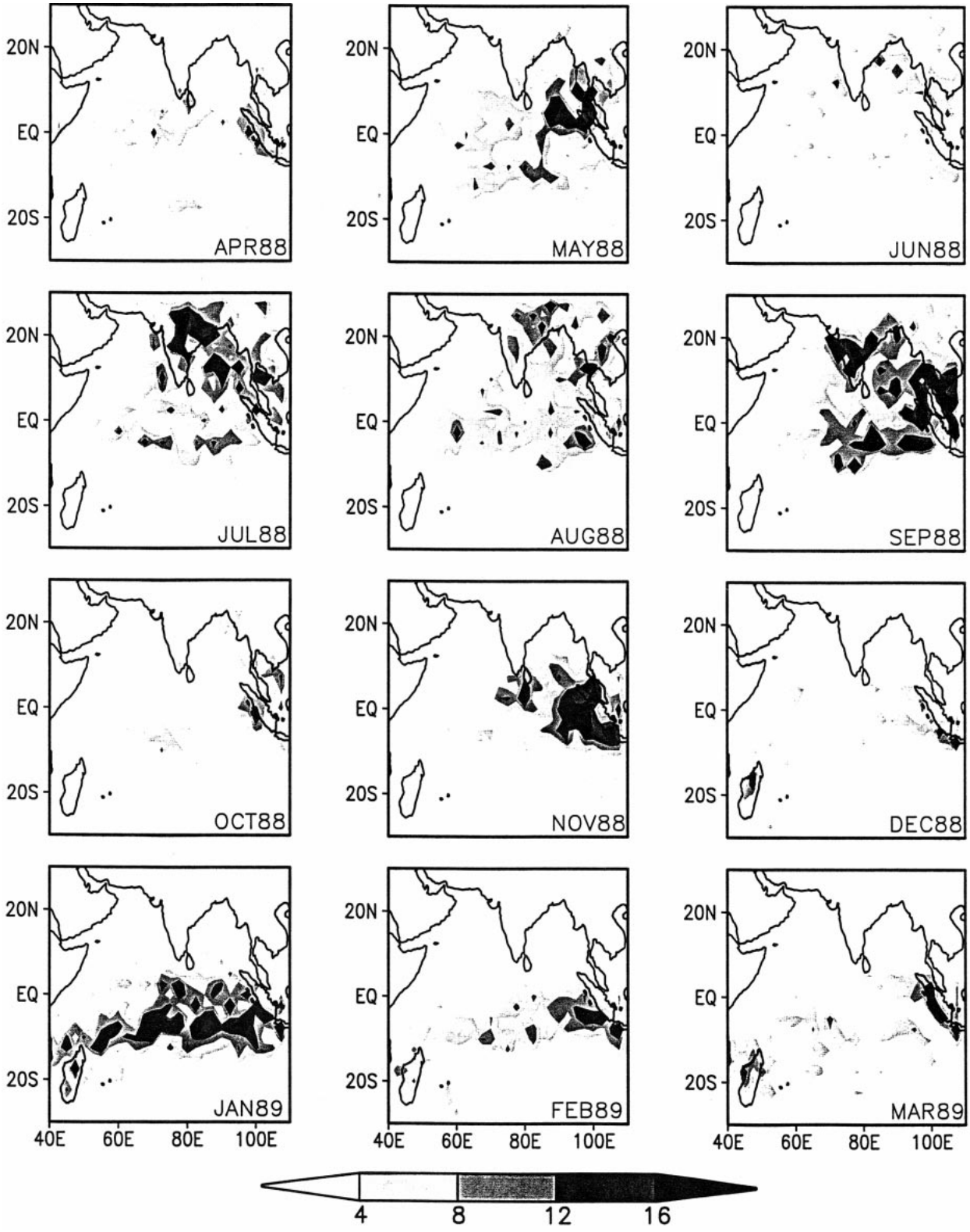

FIG. 4. Number of CSs (221 K) of at least two-image life span formed in 2.5° × 2.5° boxes.

tion. Perhaps both the dynamics and thermodynamics are important in driving the convection over the Indian region and this aspect needs further analysis.

In Fig. 4 a bimonthly modulation of the areal extent of frequent convection (i.e., four or more CSs forming in a 2.5° × 2.5° grid box in a month) is observed. On the other hand, the total number of CSs forming in the study region does not exhibit such a bimonthly variation (Fig. 6 to be discussed later). This suggests that convective activity is confined to certain areas during some months (e.g., May 1988), whereas, in the preceding or succeeding months, convection is spread over a larger area (e.g., April 1988).

An important question is, are there preferred regions of formation and dissipation of CSs? Figure 5 shows the distribution of total formed minus the total dissipated in each 2.5° × 2.5° box. The coastal belt is found to be a preferred region of formation during some months, for example, in September. In general, however, regions of net formation and net dissipation are adjacent to each other, randomly distributed without spatially large coherent zones. (When CSs of area larger than 48 400 km^2 were considered the results are found to be similar.) One reason (as will be shown later) is that majority of CSs are short lived (typically 6 h or less) and are dissipated before traveling far from their place of origin. Very long lasting CSs do travel considerable distances; however, they are relatively few in number to influence the average picture.

b. Number

Figure 6 shows the number of CSs per image for temperature thresholds from 201 to 261 K. This figure shows the number of CSs per frame without tracking (i.e., CSs in every image are treated as independent), with tracking (a CS counted only once) and those having a life cycle of at least two images. The difference between the latter two gives the number of single-frame systems. The tracked number of systems gives the information on the average number of systems forming every month, and the untracked number provides the average instantaneous picture for the month. The general features of the untracked and tracked data are similar except that the number of tracked systems are about three times lower compared to untracked systems. The numbers are comparable for all the months with no significant dependence on the season. For all three cases shown in Fig. 6, the number of CSs increases almost linearly up to about 251 K for all months. We expect the number of CSs to increase as the threshold temperature is decreased for the following reason. As stated in the introduction, in a typical MCS, the active Cb clouds occupy about 10% of the area and the remaining area is occupied by the anvil clouds whose height gradually decreases away from the deepest clouds. For the present study region, we calculated the relative areas occupied by cold pixels below different thresholds for 251-K CSs. It was found that the fractional areas were approximately 12%, 30%, 50%, and 65% at 211, 221, 231, and 241 K, respectively. The threshold temperature of 211 K corresponds to cloud tops near the 175-mb level (~13.5 km height) and are likely to be associated with Cb clouds. A CS containing a 4840 km^2 area of 211-K pixels (minimum size required to be recognized as a CS) is expected to have at 251 K an area of about 40 000 km^2. There are many CSs at 251 K having their area between 4840 and 40 000 km^2. Also, some decaying CSs do not contain convective clouds (i.e., deepest clouds). Thus, more and more of the clouds qualify as CSs when the threshold temperature is increased. The increase in the number of CSs with threshold temperature is not monotonous, however. A synoptic system (tropical cyclone, tropical convergence zone, etc.) contains several very deep CSs. As the threshold temperature is increased, CSs will start losing their individual identity and merge with the background cloud mass (temperature) of the synoptic system. The flattening tendency of the number of CSs with the threshold temperature between 251 and 261 K represents the start of this transition. During the monsoon months, this transition seems to start at 241 K itself; that is, the average height of the background cloud mass is higher.

The results in Fig. 6 are based on the criterion 1. When criterion 2 or 3 was used, it was observed that there is no noticeable change in the results. This is in agreement with the observations of Machado et al. (1998) that results are not sensitive to the criteria for identifying the successor.

It is desirable to compare the present results with those from the previous studies. A direct comparison is not possible as the minimum size of the CS tracked, the period of study, the geographic location, and the total extent of the study area differ among the studies. The only study on tracking of CSs in the Indian region is by Laing and Fritsch (1993), who studied a special class of convective systems, namely MCCs, from the equator to 40°N and 55° to 110°E. It may be noted that Laing and Fritsch (1993) do not mention the method of tracking. Laing and Fritsch (1993) documented 49 MCCs for the period April–December 1988. In our study, the number of systems having an area of at least 50 000 km^2 and a life span of two images is about 800 at the 221-K threshold, and the number with an area bigger than 100 000 km^2 is over 1000 at 241 K for the same period. Thus, there is a factor of at least 16 difference. Further, during November and December 1988, Laing and Fritsch (1993) did not find any MCC, whereas we have identified a number of CSs of MCC size in these months. Our study region is bigger; however, this alone cannot account for such a big difference. One main reason is that Laing and Fritsch (1993) required the CS to be elliptic with the ratio of major axis to minor axis not less than 0.7. This is a severe restriction and many natural clouds do not satisfy this requirement. As the num-

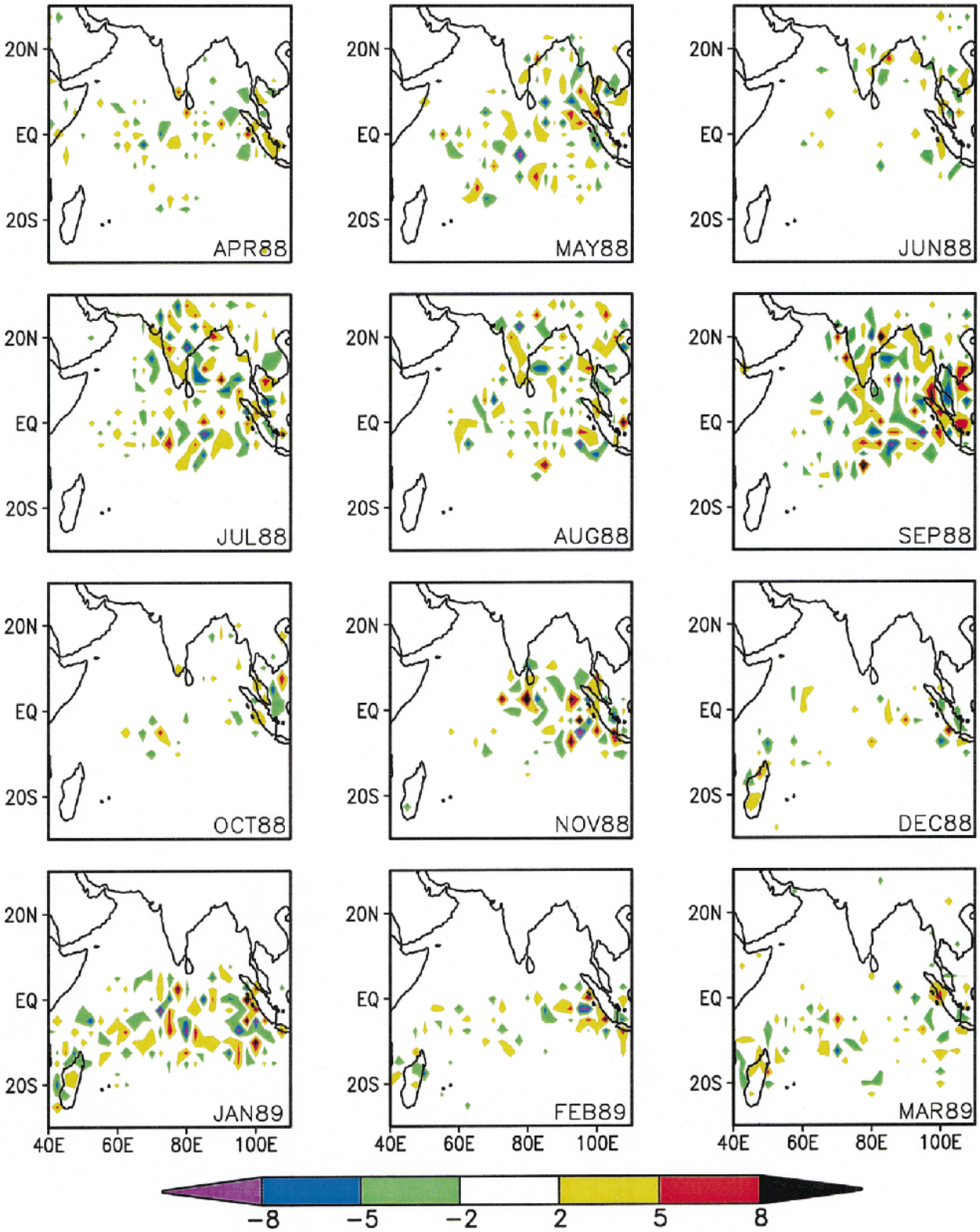

FIG. 5. Net number of CSs (221 K) formed in 2.5° × 2.5° boxes. A negative value indicates that the number of CSs that dissipated is greater when compared to that formed.

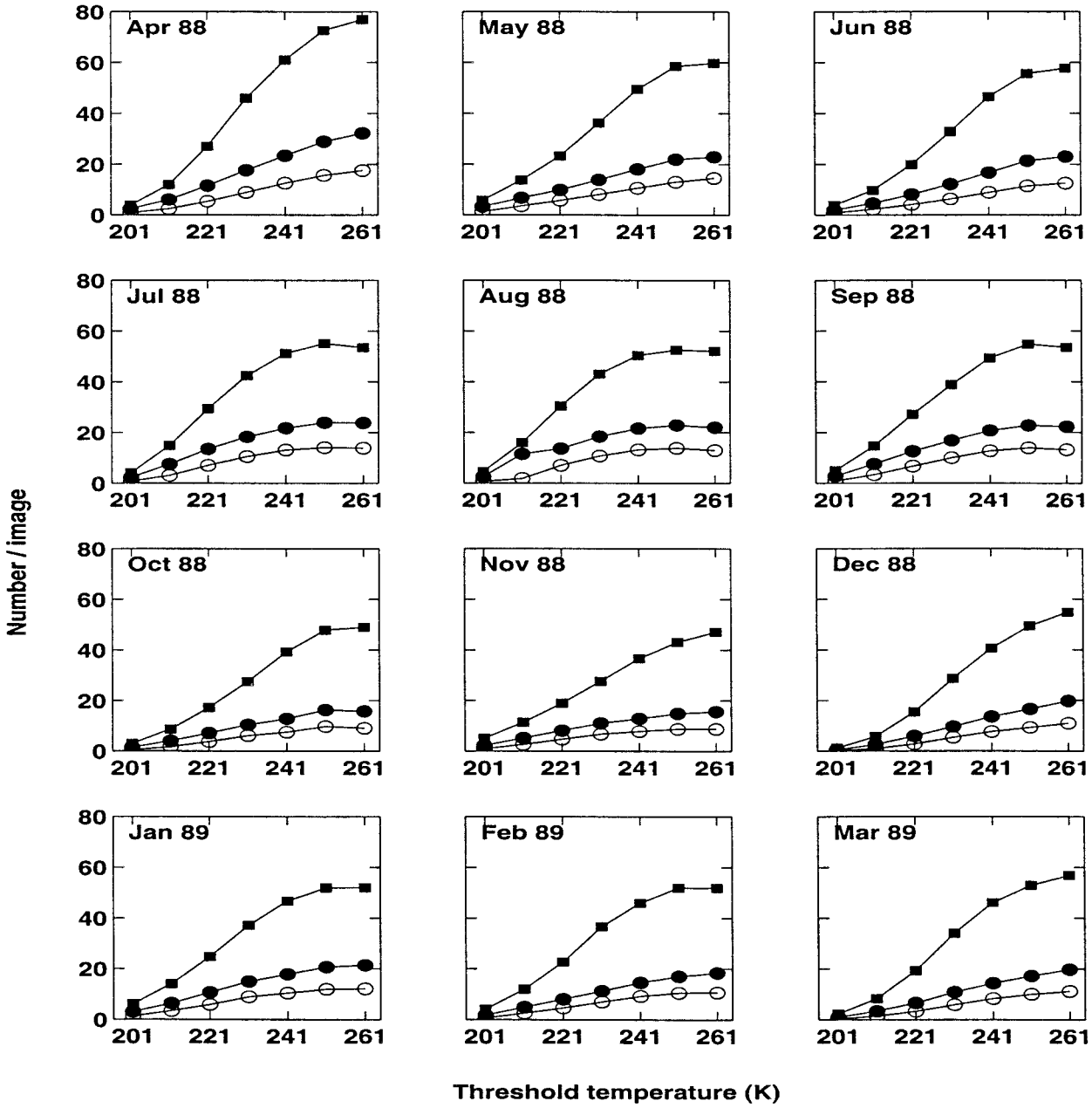

FIG. 6. Average number of CSs per image. The filled and open ovals refer to the total number of tracked systems and those having life spans of at least two images, respectively. The squares refer to the total number of systems treating clouds in every image as independent. Note that tracked number counts a long-lived system as one, even if it is present in more than one image.

ber here shows, a majority of the big systems are left out when the study is limited to MCCs only.

c. Life duration

The life span of a CS, that is, the time interval between its formation and dissipation, is an important parameter and following Laing and Fritsch (1993) is taken as $(\mathrm{nf}) \cdot (\tau)$, where nf is the number of consecutive frames/images in which the CS is present and τ is the time interval between images. Figure 7 shows the number of CSs stratified according to their life span for the month of July 1988. Figure 7a shows the dependence of the life duration on the criteria used for identifying the successor (in case the cloud splits or merges). For the short-lived systems, the life span is not sensitive to the choice of the criterion, whereas life duration of very long lived systems (more than 36 h) depends on the criteria. The longest span of the system is 168, 111, and 84 h according to criterion 1, 2, and 3, respectively. As

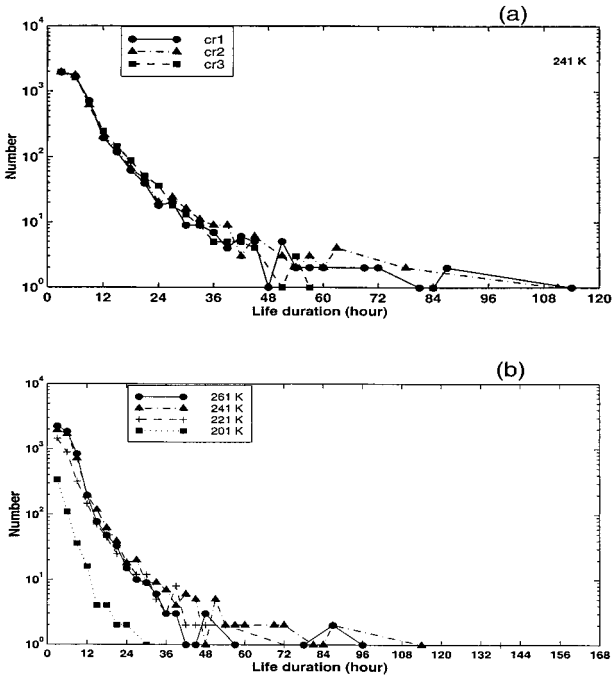

FIG. 7. Life duration distribution of CSs during Jul 1988. (a) Dependence on the successor criterion (at 241 K). (b) Dependence on threshold temperature for criterion 1.

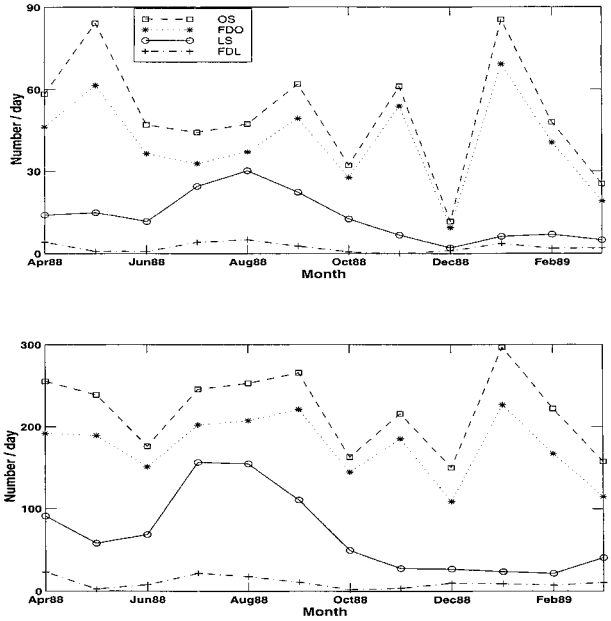

FIG. 8. Number of CSs forming over land and ocean: (a) 201 and (b) 221 K. OS, ocean systems; LS, land systems; FDO, formed and dissipated over ocean; and FDL, formed and dissipated on land.

the life of a CS increases, possibilities of splits and mergers increase and the hierarchy of the successor depends on the criterion adopted. On the other hand, for short-lived systems, splits and mergers are less frequent and hence the results are not sensitive to the criteria.

The dependence of life duration on the threshold temperature is shown in Fig. 7b. It is observed that only one system lasted for more than 24 h at 201 K, and the corresponding number is several tens at 221–261 K. The 201-K clouds (height $\sim$ 15 km) correspond to convective areas of the CSs, and others include the anvil cover. The behavior observed in Fig. 7b suggests that convective cores are short lived compared to their anvil counterparts. It was found that the deepest clouds show a strong diurnal dependence with the late evening and predawn hours as the most preferred times of growth, and morning to noon hours as most unfavorable. (A detailed study on the diurnal characteristics of CSs in the Indian region will be presented elsewhere.) While the convective cells form, grow, and decay, the anvil clouds associated with the long-lasting systems do not completely decay and maintain their identity for a longer time.

It is observed that over a range of cloud life duration, the number of systems decreases at an exponential rate; that is,

$$N(t) = N_0 e^{-\alpha t},$$

where $N(t)$ is the number of systems having a life span of t hours and N_0 and α are constants that depend on threshold temperature. The value of N_0 increases from 201 to 261 K, and α has a value between 0.2 and 0.4. Thus, short duration systems dominate the number of CSs at all temperature thresholds.

d. Land–sea contrast

Here we consider the number of systems formed and dissipated over land and ocean. A CS is called a land (ocean) system if its CG lies over land (ocean). We have seen in Figs. 4 and 5 that many systems form along the coastal belt. Coastal CSs are frequently seen to partially cover both land and ocean and assigning them to the land or ocean category is not very appropriate, but with this limitation we consider what the numbers look like. Figure 8 shows the formation and dissipation of CSs on land and ocean at threshold temperatures 201 and 221 K. The difference between those that formed and those that dissipated on land (ocean) gives the number of systems crossing the boundary and dissipating over ocean (land). It is seen that the number of CSs formed over ocean always exceeds that formed over land by a factor of 1.5–3.0. This is not surprising as oceanic area dominates in the study region. During the monsoon months (July–September), a large area over landmass is covered by convection (Fig. 3), which is reflected in Fig. 8a by the increased number of CSs forming over land. About 80% of systems formed over land dissipated over the ocean at both the threshold temperatures. The land–sea boundary is a favorite location for the formation of CSs (Fig. 4); results in Fig. 8 suggest that the majority of these CSs dissipate over the ocean. Such migration from

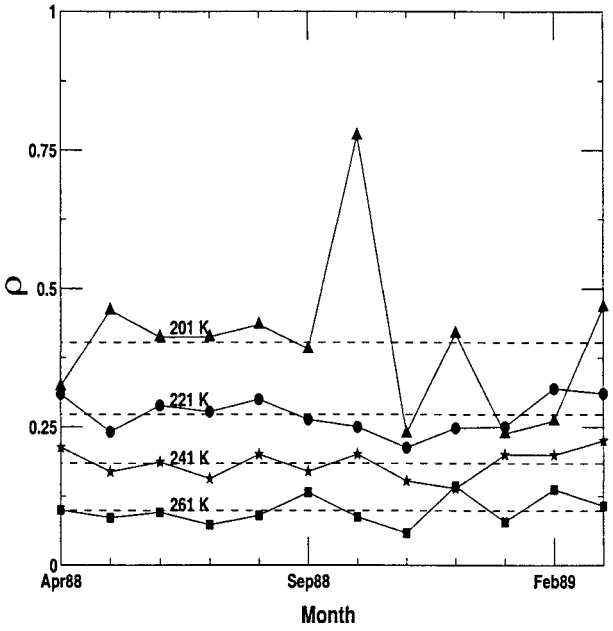

FIG. 9. Correlation coefficient ρ between life duration and maximum size of CSs at different temperature thresholds.

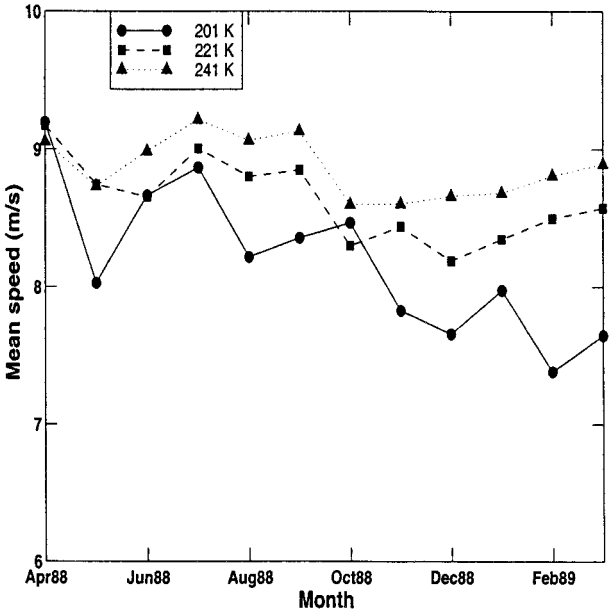

FIG. 10. Mean speeds of CSs at different temperature thresholds.

land to ocean is opposite to the movement of the synoptic systems during monsoon months that form or intensify over oceans and move over land. It may be recalled here that Nakazawa (1988) observed that the smaller systems embedded within superclusters moved opposite to the direction of superclusters. In the monsoon months there could be this possibility and this aspect is being studied.

e. Correlation between life and size

The correlation between the life duration and size of CSs is shown in Fig. 9. The maximum size attained during the life span is used in the calculation. The best correlation is found for the coldest clouds (201 K), which correspond to the convectively active area of the CS. The highest correlation of 0.8 is observed during October at the 201-K threshold. Active convective clouds are sustained by the mass of moist air converging at low levels, and the area of coldest pixels is an indicator of the strength of low-level convergence (LLC) (i.e., the amount of mass converging at low levels). While we cannot infer cause and effect solely based on correlation, a strong positive correlation between size and life span for the 201-K CSs either means that the strength of LLC increases with time or sustained LLC is maintained only if the size of the system is larger. The average correlation coefficient decreases from about 0.4 at 201 K to 0.1 at 261 K. The present correlations are in general lower than those obtained by Laing and Fritsch (1997) for global population of MCCs, where correlation ranged from 0.32 in spring to 0.57 in summer. The correlation between size and life duration can deteriorate as threshold temperature increases for many reasons. As observed in Fig. 7, the 201-K clouds are shorter lived compared to warmer clouds. As the duration of a CS increases, the chances of split and merger increase. When a big CS splits into many small CSs the correlation between size and life span decreases. At warmer threshold temperature, mainly the anvil cloud contributes to the total cloud area. The area of an anvil cloud depends on the amount of cloud mass flowing out from active clouds (which depends on the strength of LLC), how rapidly they are carried away by the winds, and how the cloud mass mixes with dry ambient air and dissipates. Thus, environmental conditions of the upper troposphere become important in addition to LLC, and correlation between size and life decreases at warmer threshold temperatures.

f. Propagation

An important feature of CSs is that they are always moving. Here the speed of propagation of a CS is calculated from the displacement of its CG. During mergers and split, large displacement of CG can take place without the actual cloudy area moving much, thus giving spuriously large speeds. Hence the average speed is calculated here only for those clouds that do not merge or split. Figure 10 shows that the average speeds vary from 7 to 9 m s^{-1}. The speeds are marginally higher during the monsoon months compared to postmonsoon months (October–December). Machado et al. (1998) observed mean speeds of propagation of 17 m s^{-1} and substantial variations from month to month. The speeds of propagation over Africa are about 12–15 m s^{-1} (Payne and McGarry 1977; Martin and Schreiner 1981). The mean

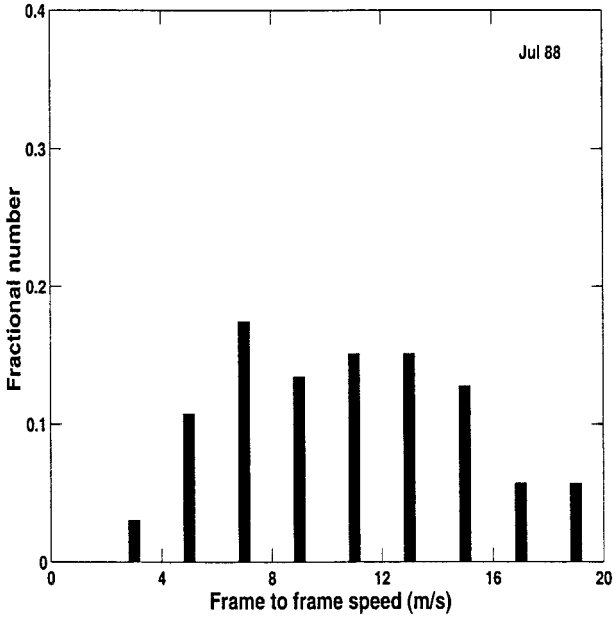

FIG. 11. Frame to frame speed distribution of CSs during Jul 1988 at 221 K.

speeds in the present study region are lower. Apart from the average speed, the speed distribution is also important and is shown in Fig. 11 for the month of July 1988 at 221 K. Figure 11 shows that the speed of propagation ranges from 2 to about 19 m s^{-1}, (the highest speed being limited due to the choice of a 200-km search box).

Machado et al. (1998) related the speeds of propagation of CSs to 750-mb wind. We explored propagations of CSs over the Indian region in relation to winds at 850-, 500-, and 200-mb levels using 12-hourly NCEP reanalysis data. It was observed that propagation of CSs appeared to be related to the ambient winds in some cases. There were cases where propagation matched 850-, 500-, or 200-mb winds. In some cases, the propagation was related to the mean of 850 and 500 mb, or the mean of 500 and 200 mb. There were also many cases where no relation was observed. This is not unexpected as previous studies have shown that the propagation of an MCS is a complex process and depends on horizontal wind speed as well as wind shear in the vertical (Barnes and Sieckman 1984).

5. Conclusions

This is the first detailed study on the life cycle and other characteristics of the deep convective CSs over the Indian region using *INSAT-1B* pixel data without constraining the clouds to specific shape factor. A new automatic algorithm to track CSs has been developed that takes into account of the mergers and splits in CSs. The algorithm is based on a combination of the maximum allowable displacement of CSs in 3 h and area overlap. The following are some important results.

1) There is a bimonthly modulation of the areal extent of convection in the region as a whole.
2) The number of CSs varies linearly with temperature threshold up to 251 K. The general features of the untracked and tracked CSs are similar except that the number of tracked systems are about three times lower compared to untracked systems.
3) About 20%–40% of CSs are found to have a one-image life span only. For the short-lived systems, the life span is not very sensitive to the choice of the criterion employed in tracking. There are differences for systems that lived for 36 h or more. Also, the life spans of CSs are less sensitive to the temperature threshold between 221 and 261 K.
4) The mean speeds of propagation of CSs vary in a narrower range of 7 to 9 m s^{-1}, which is much lower when compared to those of Atlantic systems.

Acknowledgments. This work was supported by a grant from the Indian Space Research Organization and we thank the agency for their support. We also thank Prof. J. Srinivasan for several discussions and useful suggestions. We are grateful to Prof. V. Ramanathan (Scripps Institute of Oceanography, San Diego, CA) for his advice on the use of the data.

REFERENCES

Aspliden, C. L., Y. Tourre, and J. B. Sabine, 1976: Some climatological aspects of West African disturbance lines during GATE. *Mon. Wea. Rev.,* **104,** 1029–1035.

Augustine, J. A., and K. W. Howard, 1988: Mesoscale convective complexes over the United States during 1985. *Mon. Wea. Rev.,* **116,** 685–701.

Barnes, G. M., and K. Sieckman, 1984: The environment of fast and slow moving tropical mesoscale convective cloud lines. *Mon. Wea. Rev.,* **112,** 1782–1794.

Chen, S. S., and R. A. Houze, 1997: Diurnal variation and life-cycle of deep convective systems over the tropical Pacific warm pool. *Quart. J. Roy. Meteor. Soc.,* **123,** 357–388.

Corfidi, S. F., J. H. Merritt, and J. M. Fritsch, 1996: Predicting the movement of mesoscale convective complexes. *Wea. Forecasting,* **11,** 41–46.

Duvel, J. P., 1989: Convection over tropical Africa and the Atlantic Ocean during northern summer. Part I: Interannual and diurnal variations. *Mon. Wea. Rev.,* **117,** 2782–2799.

Evans, J. L., and R. E. Shemo, 1996: A procedure for automated satellite-based identification and climatology development of various cases of organized convection. *J. Appl. Meteor.,* **35,** 638–652.

Fu, R., A. D. Del Genio, and W. B. Rossow, 1990: Behavior of deep convective clouds in the tropical Pacific deduced from ISCCP radiances. *J. Climate,* **3,** 1129–1152.

——, ——, and ——, 1994: Influence of ocean surface conditions on atmospheric vertical thermodynamic structure and deep convection. *J. Climate,* **7,** 1092–1108.

Gadgil, S., P. V. Joseph, and N. V. Joshi, 1984: Ocean–atmosphere coupling over monsoon regions. *Nature,* **312,** 141–143.

Graham, N. E., and T. P. Barnett, 1987: Sea surface temperature, surface wind divergence and convection over tropical oceans. *Science,* **238,** 657–659.

Hall, T. J., and T. H. Vonder Haar, 1999: The diurnal cycle of west Pacific deep convection and its relation to the spatial and temporal variation of tropical MCSs. *J. Atmos. Sci.*, **56,** 3401–3415.

Houze, R. A., Jr., 1989: Observed structure of mesoscale convective systems and implications for large-scale heating. *Quart. J. Roy. Meteor. Soc.,* **115,** 425–461.

——, 1993: *Clouds Dynamics.* Academic Press, 573 pp.

——, and C. Cheng, 1977: Radar characteristics of tropical convection observed during GATE: Mean properties and trends over the summer season. *Mon. Wea. Rev.,* **105,** 964–980.

Laing, A. G., and J. M. Fritsch, 1993: Mesoscale convective complexes over the Indian monsoon region. *J. Climate*, **6,** 911–919.

——, and ——, 1997: The global population of mesoscale convective complexes. *Quart. J. Roy. Meteor. Soc.,* **123,** 389–405.

Ludlam, F. H., 1980: *Clouds and Storms: The Behavior and Effect of Water in the Atmosphere.* The Pennsylvania State University Press, 405 pp.

Machado, L. A. T., and W. B. Rossow, 1993: Structural characteristics and radiative properties of tropical cloud clusters. *Mon. Wea. Rev.,* **121,** 3234–3260.

——, ——, R. L. Guedes, and A. W. Walker, 1998: Life cycle variations of mesoscale convective systems over the Americas. *Mon. Wea. Rev.,* **126,** 1630–1654.

Maddox, R. A., 1980: Mesoscale convective complexes. *Bull. Amer. Meteor. Soc.,* **61,** 1374–1387.

Mapes, B. E., and R. A. Houze Jr., 1993: Cloud clusters and super clusters over the oceanic warm pool. *Mon. Wea. Rev.,* **121,** 1398–1415.

——, and ——, 1995: Diabatic divergence profiles in western Pacific mesoscale systems. *J. Atmos. Sci.,* **52,** 1807–1828.

Martin, D. W., and A. J. Schreiner, 1981: Charecteristics of west African and east Atlantic cloud clusters a survey from GATE. *Mon. Wea. Rev.,* **109,** 1671–1688.

Mohr, K. I., and E. J. Zipser, 1996: Mesoscale convective systems defined by their 85-GHz ice scattering signature: Size intensity comparison over tropical oceans and continents. *Mon. Wea. Rev.,* **124,** 2417–2437.

Nakazawa, T., 1988: Tropical super clusters within intra seasonal variations over the western Pacific. *J. Meteor. Soc. Japan,* **66,** 823–839.

Payne, S. W., and M. M. McGarry, 1977: The relationship of satellite infrared convective activity to easterly waves over West Africa and the adjacent ocean during phase III of GATE. *Mon. Wea. Rev.,* **105,** 413–420.

Slutz, R. J., S. J. Lubker, J. D. Hiscox, S. D. Woodruff, R. L. Jenne, D. H. Joseph, P. M. Steurer, and J. D. Elms, 1985: COADS: Comprehensive Ocean–Atmosphere Data Set. Release 1, NOAA, 262 pp. [Available from Climate Research Program, Environmental Research Laboratory, NOAA, Boulder, CO 80303.]

Webster, P. J., and G. L. Stephens, 1980: Tropical upper-tropospheric extended clouds: Inferences from Winter Monex. *J. Atmos. Sci.,* **37,** 1521–1541.

Williams, M., and R. A. Houze Jr., 1987: Satellite-observed characteristics of winter monsoon cloud clusters. *Mon. Wea. Rev.,* **115,** 505–519.